Phase Transformation Theory: A Powerful Tool for the Design of Advanced Steels

F.G. Caballero, M.K. Miller, C. Garcia-Mateo, C. Capdevila, and C. Garcia de Andrés

Enhanced for the Web

This article appears on the JOM *web site* ***(www.tms.org/jom.html)*** *in html format and includes links to additional on-line resources.*

An innovative design procedure based on phase transformation theory alone has been successfully applied to design steels with a microstructure consisting of a mixture of bainitic ferrite, retained austenite, and some martensite. An increase in the amount of bainitic ferrite is needed in order to avoid the presence of large regions of untransformed austenite, which under stress decompose to brittle martensite. The design procedure addresses this difficulty by adjusting the T_o' curve to greater carbon concentrations with the use of substitutional solutes such as manganese and chromium. The concepts of bainite transformation theory can be exploited even further to design steels with strength in excess of 2.5 GPa and considerable toughness.

INTRODUCTION

The thermomechanical control processed bainitic steels have not been as successful as those that are quenched and tempered because of the presence of coarse cementite particles in the bainitic microstructure. The addition of ~2 wt.% silicon to such a steel enables the production of a distinctive microstructure consisting of a mixture of bainitic ferrite, carbon-enriched retained austenite, and some martensite. The silicon suppresses the precipitation of brittle cementite during bainite formation, and hence should lead to an improvement in toughness. The essential principles governing the optimization of such microstructures are well established. In particular, an increase in the amount of bainitic ferrite in the microstructure is needed in order to consume large regions of untransformed austenite, which under stress decompose to hard, brittle martensite.[1,2] In this sense, the aim of this work is the design, using phase transformation theory, of a series of carbide-free bainitic steels with improved properties of strength, ductility, and toughness for high-performance application.

How would you…

…describe the overall significance of this paper?

An innovative design procedure based on phase transformation theory has been successfully applied to design a new generation of ultra-high-strength steels with desirable levels of toughness, properties that have awakened great interest in the technical and scientific community. The excellent properties achieved are mainly a consequence of the formation of bainitic ferrite plates just a few nanometers thick. Temperatures at which iron diffusion during bainite transformation occurs are inconceivable. In that sense, the microstructure and its characterization at an atomic level represent a scientific milestone.

…describe this work to a materials science and engineering professional with no experience in your technical specialty?

The alloys designed in this work present the highest strength/toughness combinations ever recorded in bainitic steels. These alloys show better mechanical properties of the quenched and tempered low-alloy martensitic steels and match the critical properties of maraging steels, which are at least thirty times more expensive. Moreover, this work has revealed that bainite can be obtained by transforming at very low temperatures. This has the consequence that the plates of bainite are fine-scale, 20–40 nm thick, so that the material becomes very strong.

…describe this work to a layperson?

A simple, ingenious, and inexpensive way of producing a very strong steel has been developed. This new form of steel is called NANOBAIN. It is incredibly strong and tough. This is because it contains crystals which are only a few billionths of a meter in thickness. The fine crystals are generated at relatively low temperature, no hotter than those needed to cook a pizza. NANOBAIN is a material with a promising future.

Phase Transformation Models in Steels

The bainite transformation progresses by the diffusionless growth of tiny platelets known as sub-units.[3] The excess carbon in these platelets partitions into the residual austenite soon after the growth event. Diffusionless growth of this kind can only occur if the carbon concentration of the residual austenite is below that given by the T_o curve. The T_o curve is the locus of all points, on a temperature-versus-carbon concentration plot, where austenite and ferrite of the same chemical composition have the same free energy.[4] The T_o' curve is defined similarly but takes into account the stored energy of the ferrite due to the displacive mechanism of transformation. It follows that the maximum amount of bainite that can be obtained at any temperature is limited by the fact that the carbon content of the residual austenite must not exceed the T_o curve of the phase diagram. The design procedure avoids this difficulty in two ways: by adjusting the T_o curve to greater carbon concentrations with the use of substitutional solutes and by controlling the mean carbon concentration.[1,2]

Bainite is formed below the T_o'

Table I. Actual Chemical Composition of Designed Advanced Bainitic Steels (in wt.%)

Steel	C	Si	Mn	Ni	Cr	Mo	V
First Set of Alloys							
Ni1	0.31	1.51	<0.01	3.52	1.44	0.25	0.10
Ni2	0.30	1.51	<0.01	3.53	1.42	0.25	—
Second Set of Alloys							
CENIM 1	0.29	1.50	2.25	—	—	0.26	—
CENIM 2	0.29	1.46	1.97	—	0.46	0.25	—
CENIM 3	0.29	1.49	1.56	—	1.47	0.25	—
CENIM 4	0.27	1.71	1.53	1.47	0.17	0.24	—
Low-Temperature Bainite							
NANOBAIN	0.98	1.46	1.89	—	1.26	0.26	0.09
(at. %)	(4.34)	(2.76)	(1.82)	—	(1.28)	(0.14)	(0.09)

temperature when $\Delta G^{\gamma\rightarrow\alpha} < -G_{SB}$ and $\Delta G_m < G_N$, where $G_{SB} \cong 400$ J mol^{-1} is the stored energy of bainite[4] and $\Delta G^{\gamma\rightarrow\alpha}$ is the free energy change accompanying the transformation of austenite without any change in chemical composition. The first condition therefore describes the limit to bainite growth. The second condition refers to nucleation; thus, ΔG_m is the maximum molar Gibbs free energy change accompanying the nucleation of bainite. G_N is a universal nucleation function based on a dislocation mechanism of the kind associated with martensite.[5] The temperature dependence of G_N is independent of chemical composition; together with the growth condition, the function allows the calculation of the bainite start temperature, B_s, from a knowledge of thermodynamics alone.

Apart from controlling the T_o' curve and B_s temperature, substitutional solutes also affect hardenability, which is an important design parameter to avoid transformations such as proeutectoid ferrite and pearlite. For this purpose, thermodynamic and kinetics models developed to allow the estimation of isothermal and continuous transformation diagrams, from a knowledge of the chemical composition of the steel concerned, were used in the design process.[6–10] The output parameters of the models are: t_{dif}, which is the minimum time at the ferrite and pearlite nose in the time-temperature-transformation (TTT) diagram; t_{displ}, which represents the minimum time at the bainitic nose in the TTT diagram; and V_b, which indicates the maximum volume fraction of bainite formed at a given transformation temperature according to the T_o' curve. There are other output parameters such as the martensite and Widmanstätten start temperatures.

DESIGN OF ADVANCED BAINITIC STEELS

In previous research carried out by H.K.D.H. Bhadeshia and D.V. Edmonds[1,2] and V.T.T. Miihkinen and D.V. Edmonds,[11–13] it was found that carbide-free bainite is in principle an ideal microstructure from many points of view. In particular, the steel has a high resistance to cleavage fracture and void formation due to the absence of fine carbides. There is a possibility of simultaneously improving strength and toughness because of the ultrafine grain size of the bainitic ferrite plates, and of further enhancing the toughness by a transformation-induced plasticity effect.

These original experiments[1,2] were carried out in order to demonstrate the role of the T_o curve in greatly influencing the mechanical properties of carbide-free bainitic steels. The experimental alloys developed for this purpose are not necessarily the optimum alloys from the point of view of mechanical properties. The aim was to use the combination of the models mentioned above to produce the best possible alloys, with microstructures produced by continuous cooling transformation, building on the previous work.[1,2]

First Set of Designed Bainitic Steels Containing Nickel

The first set of alloys proposed following a very large number of theoretical investigations are listed in Table I. The alloys contain Ni, V, and Cr for hardenability, Si to prevent the precipitation of cementite during bainite formation, and Mo to prevent temper embrittlement due to P in the alloy. In order to reach high strength (1,100

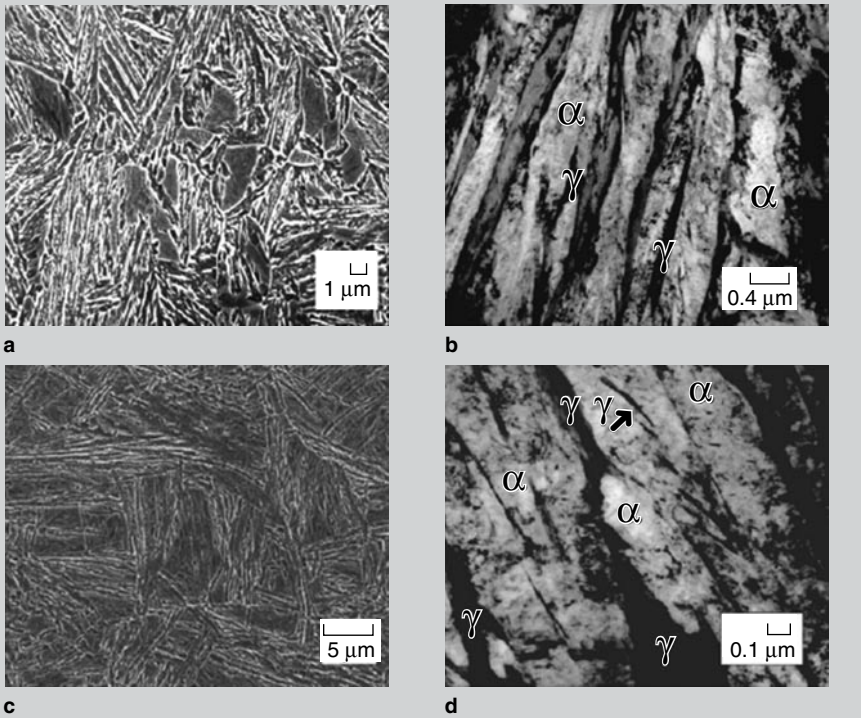

Figure 1. Scanning and transmission electron micrographs of the designed steels: (a, b) Ni1, (c, d) Ni2. α is bainitic ferrite and γ is retained austenite.

Table II. Quantitative Data on Microstructure and Hardness of the Designed Steels

Steel / FCT	V_B	V_M	V_γ	x_γ (wt.%)	HV30
Ni2 (Reference)	0.81 ± 0.06	0.08 ± 0.05	0.11 ± 0.01	1.03 ± 0.03	536 ± 6
CENIM 1 / 450ºC	0.73 ± 0.04	0.24 ± 0.05	0.03 ± 0.01	0.66 ± 0.06	530 ± 7
CENIM 1 / 600ºC	0.76 ± 0.03	0.21 ± 0.04	0.03 ± 0.01	0.95 ± 0.01	522 ± 4
CENIM 2 / 500ºC	0.77 ± 0.04	0.13 ± 0.05	0.10 ± 0.01	1.14 ± 0.03	519 ± 3
CENIM 2 / 550ºC	0.80 ± 0.04	0.09 ± 0.05	0.10 ± 0.01	1.26 ± 0.07	460 ± 20
CENIM 3 / 500ºC	0.88 ± 0.02	0.02 ± 0.03	0.11 ± 0.01	1.03 ± 0.05	495 ± 15
CENIM 3 / 550ºC	0.86 ± 0.02	0.03 ± 0.04	0.11 ± 0.01	1.04 ± 0.04	505 ± 6
CENIM 4 / 500ºC	0.88 ± 0.02	0.09 ± 0.04	0.03 ± 0.01	1.26 ± 0.07	531 ± 10

FCT is interrupted accelerating cooling temperature; V_B is the volume fraction of bainitic ferrite; V_M is the volume fraction of martensite; V_γ is the volume fraction of austenite; x_γ is the carbon content in austenite.

MPa as minimum), the amount of carbon was selected to be 0.3 wt.% carbon in the three designed alloys. Calculated TTT and continuous cooling transformation (CCT) diagrams suggested that proposed alloys had enough hardenability to avoid transformations such as proeutectoid ferrite and pearlite, if the steel is cooled in air after conventional thermomechanical processing. In that case, the final microstructure in the designed steels was predicted to be fully bainitic.[14]

Designed steels were prepared as 35 kg vacuum induction melts. Ingots were forged down to a thickness of 25 mm before their temperature fell below 750ºC. Microstructural characterization revealed that the nickel alloyed steels in Table I had the desired microstructure consisting of carbide-free upper bainite (α phase) with interlath high carbon (~1 wt.% carbon) retained austenite films (γ phase) (Figure 1).[15] The two steels achieved the highest combination of strength and toughness for bainitic microstructures. Toughness values of nearly 130 MPa $m^{1/2}$ were obtained for strength in the range of 1,600–1,700 MPa.[15] This work demonstrated experimentally that models based on phase transformation theory can be successfully applied to the design of carbide-free bainitic steels.

Newly Designed Bainitic Steels Containing Manganese

More recently, a new set of alloys was designed to have the same bainitic transformation region in the TTT diagram and the same T_o' curve as those of Ni2 bainitic steel,[16] while avoiding nickel additions for economic reasons. The chemical composition of the new alloys was selected to have t_{displ} and V_b at 400ºC similar to those of Ni2 steel. Both parameters define bainite transformation according to thermodynamics.[7] Moreover, t_{dif} must be high enough to avoid the formation of proeutectoid ferrite during cooling. The chemical compositions of the new designed steels are given in Table I. Calculated TTT diagrams suggested that a two-step cooling schedule is the most promising processing route to obtain a full bainitic microstructure in the new alloys. An initial rapid cooling (at least 30ºC/s) should be performed to avoid the formation of proeutectoid ferrite during cooling. The cooling rate should be decreased (around 0.5ºC/s) before B_s temperature is reached (around 500ºC), in order to cross the bainitic zone of the TTT diagram. According to the kinetic model, a full bainitic microstructure (volume fraction of bainite higher than 0.75) will be formed by applying this two-step cooling schedule after finishing rolling.

The proposed alloys were prepared in a 60 kg vacuum induction furnace. Samples were hot rolled to ~12 mm in several passes, finishing at 930ºC. The desired bainitic microstructure was obtained in all the steels by air cooling from different temperatures after an initial accelerated cooling at 70ºC/s. Experimental data on the microstructure are presented in Table II. Scanning and transmission electron micrographs (SEM and TEM) of fully carbide-free bainitic microstructures (more than 75% of bainitic ferrite) in the four designed steels are shown in Figure 2. Microstructural characterization revealed that the CENIM 1–4 alloys, after air cooling from every temperature tested, have the desired microstructure consisting of carbide-free upper bainite. Due to the high volume fraction of bainitic ferrite in those samples, retained austenite is present as films between the subunits of bainitic ferrite. Both phases are free of carbides, as the TEM micrographs confirm.

The corresponding mechanical properties are reported in Table III together with those for the reference material (Ni2 steel). The values presented are the averages of three tests. The tensile tests were performed at room temperature and low strain rate (0.008 s^{-1}). Plates of bainitic ferrite are typically 10 μm long and ~0.2 μm thick (see the TEM micrographs in Figure 2). This morphology gives a small mean free path for dislocation glide. Thus, the main microstructural contribution to the strength of bainite is from the extremely fine grain size of bainitic ferrite. It is difficult to separate the effect of retained austenite on the strength of these steels from other factors. Qualitatively, austenite can affect the strength in several ways. Residual austenite can transform to martensite during cooling to room temperature.[11,12] In addition, retained austenite interlath films can increase the strength by transforming to martensite during testing, similar to

Table III. Tensile Properties and Charpy Impact Test Results at 20ºC

Steel/FCT	YS (MPa)	UTS (MPa)	TE (%)	Impact Energy (J)
Ni2 (Reference)	1,054 ± 49	1,523 ± 21	25 ± 1	50 ± 1
CENIM 1/ 450ºC	1,240 ± 31	1,796 ± 21	18 ± 1	36 ± 2
CENIM 1/ 600ºC	1,204 ± 29	1,701 ± 9	16 ± 1	22 ± 1
CENIM 2/ 500ºC	1,187 ± 16	1,606 ± 30	17 ± 2	36 ± 2
CENIM 2/ 550ºC	1,128 ± 32	1,539 ± 21	16 ± 2	44 ± 2
CENIM 3/ 500ºC	1,194 ± 35	1,652 ± 6	18 ± 1	44 ± 1
CENIM 3/ 550ºC	1,204 ± 18	1,642 ± 12	18 ± 1	46 ± 2
CENIM 4/ 500ºC	1,339 ± 16	1,763 ± 18	16 ± 1	38 ± 1

FCT is interrupted accelerating cooling temperature; YS yield strength; UTS ultimate tensile strength; TE total elongation.

the behavior of transformation-induced plasticity steels.[11,12] Tensile elongation is controlled by the volume fraction of retained austenite. Retained austenite is a ductile phase compared to the bainitic ferrite and would be expected to enhance ductility provided the austenite is homogeneously distributed along plate boundaries (film austenite). However, isolated pools of austenite (blocky austenite) would have an unfavorable result on both elongation and strength. From Table III, it is clear that the steels possess a combination of high strength and good ductility.

Impact toughness was measured on normalized Charpy notched (10 mm² × 10 mm²) samples at 20ºC with the use of a 300 J Charpy testing machine. Charpy impact test results are also listed in Table III for all alloys. A considerable improvement in toughness is obtained when the volume fraction of bainite increases in the microstructure. The results are consistent with the enhancement of toughness expected when the amount of blocky austenite and martensite are reduced and, in general, when the thermal and mechanical stability of residual austenite is increased.

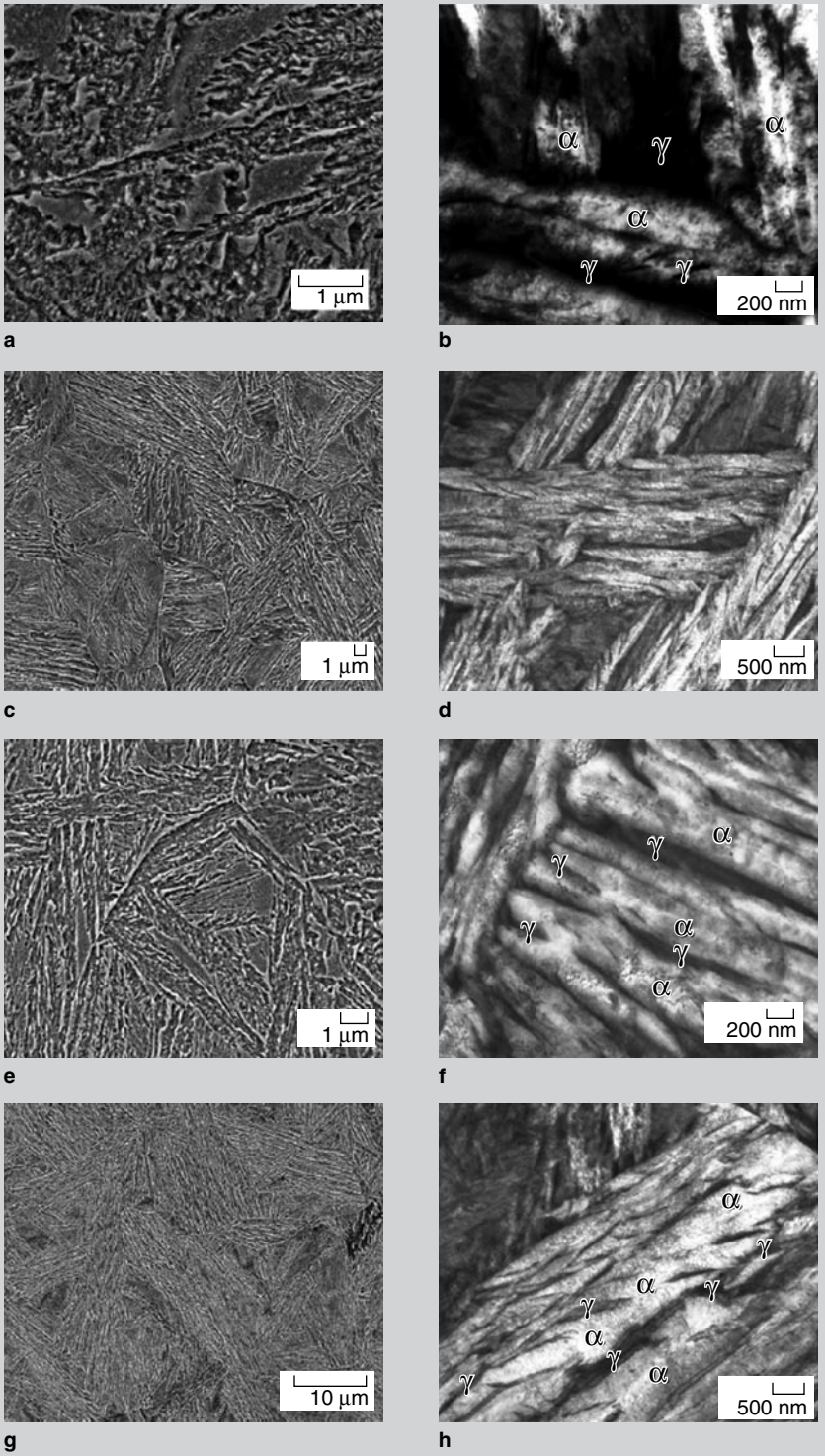

Figure 2. Scanning and transmission electron micrographs of the designed steels after air cooling from different temperatures: (a, b) CENIM 1 / 600ºC, (c, d) CENIM 2 / 550ºC, (e, f) CENIM 3 / 500ºC, (g, h) CENIM 4 / 500ºC. α is bainitic ferrite and γ is retained austenite.

Low-Temperature Bainite: From Micro to Nano

A combination of the models described above was used to produce the finest possible bainitic microstructure by transformation at the lowest possible temperature. From the models, NANOBAIN steel (Table I) was proposed to decrease bainite transformation temperatures, increase the maximum volume fraction of bainite in the final microstructure, and to improve the hardenability of the steels. The carbon concentration was selected from calculations to suppress B_s temperature and to make austenite stronger, with the aim of obtaining extremely thin platelets of bainite. Samples were supplied as 30 kg cast ingots. They were first homogenized at 1,200ºC for two days in partially evacuated quartz capsules flushed with argon. Afterward, the sealed samples were cooled in air. The homogenized specimens were then austenitized for 15 min. at 1,000ºC, and isothermally transformed at temperatures ranging

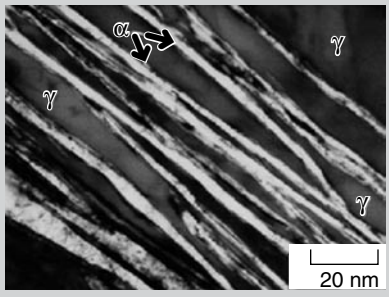

Figure 3. A transmission electron micrograph of a microstructure obtained at 200ºC for 15 days in NANOBAIN steel. α is bainitic ferrite and γ is retained austenite.

from 125ºC to 500ºC for different times before quenching into water.

A transmission electron micrograph of NANOBAIN transformed at 200ºC for 15 days is presented in Figure 3. Some of the plates of bainite are incredibly thin (20–40 nm) and long, giving a fine scale structure consisting of an intimate mixture of austenite and ferrite. Dislocation debris is evident in both the bainitic ferrite and the surrounding austenite. Extensive TEM failed to identify carbides in the microstructure; only a few extremely fine (20 nm wide and 175 nm long) cementite particles in the bainitic ferrite were found in samples transformed at 190ºC for 14 days.[17] Quite remarkably, the bainite plates formed at 200ºC (Figure 3) have a width that is less than 50 nm, with each plate separated by an even finer film of retained austenite. The small thickness of bainitic ferrite plates in low-temperature bainite leads to hardness values in excess of 600 HV and strengths in excess of 2.5 GPa.[17]

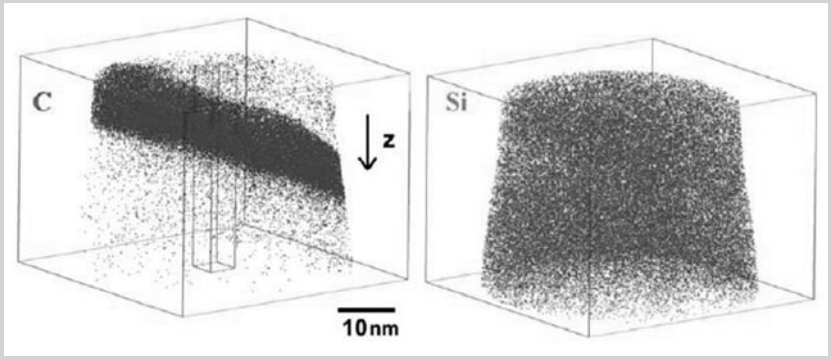

a b

Figure 4. (a) Carbon and (b) silicon atom maps showing a cementite particle precipitated inside bainitic ferrite in sample transformed at 200ºC for 10 days.

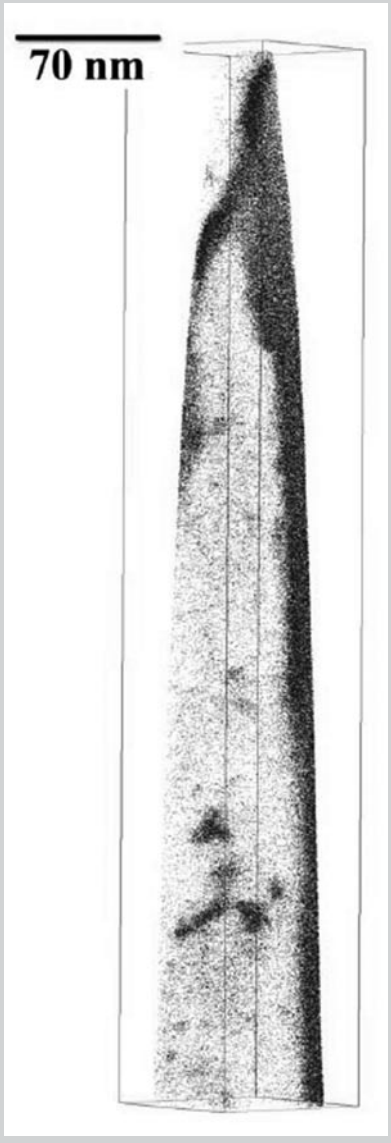

a

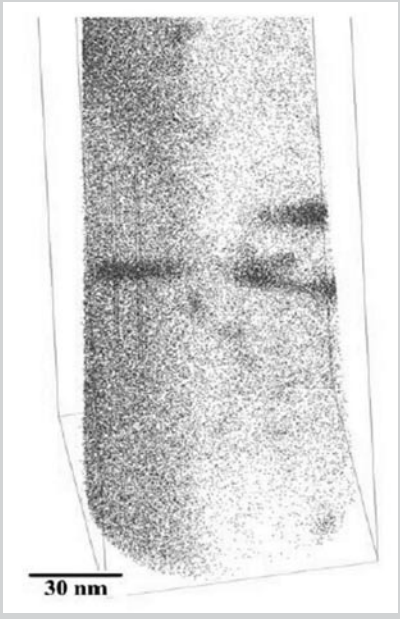

b

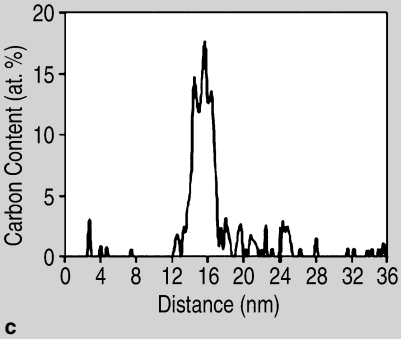

c

Figure 5. A carbon atom map (a) showing carbon clusters in bainitic ferrite after tempering at 400ºC for 30 min.; the enlarged region (b) has been rotated to show the analysis volume used for the concentration profile (c) across a carbon cluster.

Theory indicates that the largest effect of bainite plate thickness is due to the strength of the austenite, the free energy change accompanying transformation, and a small independent effect due to transformation temperature.[18] In this case, the observed refinement is mainly a consequence of the effect of high carbon content and the low transformation temperature on increasing the strength of the austenite.

Initially, transmission electron microscopy was unable to reveal carbide particles inside the bainitic ferrite; however, after a large and equivalent set of accumulated atom probe results, the presence of cementite has been confirmed as the lower bainite carbide despite the high carbon and high silicon content of the steel used. An example of carbide particle precipitated inside bainitic ferrite for a sample transformed at 300ºC for 8 hours is shown in carbon and silicon atoms maps in Figure 4 from atom probe measurements. The measured carbon level (~25 at.%) allows the type of carbide precipitated inside bainitic ferrite to be identified as cementite (i.e., 25 at.% for cementite versus 30 at.% for ε-carbide). It is clear from these results that para-cementite is observed (i.e., cementite formed with the same Fe/M atom ratio as the matrix, where M is a substitutional atom such as silicon).[19] Since silicon does not partition and is expected to favor the precipitation of ε-carbide, the absence of ε-carbide precipitation in this high-carbon bainitic steel can be only rationalized in terms of carbon trapping at dislocations as in the theory of tempering due to Kalish and Cohen.[20] Atom probe tomography also revealed that this ex-

cess of carbon was trapped at dislocations in the vicinity of the ferrite/austenite interface. As a result, the carbide precipitation sequence is modified.[21] Moreover, carbon atom maps and concentration profiles of bainite at early stages of tempering (400ºC for 30 min.) clearly show the presence of carbon-enriched regions, randomly dispersed throughout a carbon-depleted ferrite matrix, as presented in Figure 5. These clusters are ~6 nm thick and have a maximum carbon content of ~14 at.%. Such fluctuations of solute concentration may be associated with the solute redistribution to dislocations in bainite, as explained above. These regions may be gradually replaced by regions even more highly enriched in carbon, signifying the onset of ε-carbide precipitation as the tempering temperature is increased.[22]

CONCLUSIONS

The alloys designed in this work present the highest strength/toughness combinations ever recorded in bainitic steels. These alloys show better mechanical properties of the quenched and tempered low-alloy martensitic steels and match the critical properties of maraging steels, which are at least thirty times more expensive. Moreover, this work has revealed that it is possible to obtain bainite by transforming at very low temperatures. This has the consequence that the plates of bainite are fine-scale, 20–40 nm thick, so that the material becomes very strong. When this feature is combined with the fact that the plates of ferrite are interspersed with austenite, it becomes possible to create strong and tough steels. Although the results themselves are exciting, the potential for commercial exploitation is large because the alloys are very inexpensive and easy to manufacture.

ACKNOWLEDGEMENT

The authors gratefully acknowledge the support of Spanish Ministerio de Ciencia y Tecnología Plan Nacional de I+D+I (2004–2007) funding this research under the contract MAT2007–63873. All of the authors want to thank Arcelor Research for manufacturing the designed alloys. Research at the Oak Ridge National Laboratory SHaRE User Facility was sponsored by the Scientific User Facilities Division, Office of Basic Energy Sciences, U.S. Department of Energy. The authors also would like to express their special acknowledgement to Prof. H.K.D.H. Bhadeshia for helpful discussions.

References

1. H.K.D.H. Bhadeshia and D.V. Edmonds, *Met. Sci.*, 17 (1983), pp. 411–419.
2. H.K.D.H. Bhadeshia and D.V. Edmonds, *Met. Sci.*, 17 (1983), pp. 420–425.
3. H.K.D.H. Bhadeshia and D.V. Edmonds, *Acta Metall.*, 28 (1980), pp. 1265–1273.
4. H.K.D.H. Bhadeshia, *Acta Metall.*, 29 (1981), pp. 1117–1130.
5. C. García-Mateo and H.K.D.H. Bhadeshia, *Mat. Sc. and Eng.*, 378A (2004), pp 289–292.
6. Materials Algorithms Project (MAP), Department of Materials Science and Metallurgy, University of Cambridge, U.K.: *http://www.msm.cam.ac.uk/map*.
7. H.K.D.H. Bhadeshia, *Met. Sci.*, 16 (1982), pp. 159–165.
8. S.J. Jones and H.K.D.H. Bhadeshia, *Acta Metall.*, 45 (1997), pp. 2911–2920.
9. S.V. Parker, "Modelling of Phase Transformation in Hot Rolled Steels" (Ph.D. thesis, University of Cambridge, U. K., 1997).
10. F.G. Caballero, C. Capdevila, and C. García de Andrés, *Mat. Sci. Technol.*, 18 (2002), pp. 534–540.
11. V.T.T. Miihkinen and D.V. Edmonds, *Mater. Sci. Technol.*, 3 (1987), pp. 422–431.
12. V.T.T. Miihkinen and D.V. Edmonds, *Mater. Sci. Technol.*, 3 (1987), pp. 432–440.
13. V.T.T. Miihkinen and D.V. Edmonds, *Mater. Sci. Technol.*, 3 (1987), pp. 441–449.
14. F.G. Caballero et al., *Mat. Sci. and Technol.*, 17 (2001), pp. 512–516.
15. F.G. Caballero et al., *Mat. Sci. and Technol.*, 17 (2001), pp. 517–522.
16. F.G. Caballero et al., *ISIJ Inter.*, 46 (7) (2006), pp. 1479–1488.
17. F.G. Caballero et al., *Mater. Sci. Technol.*, 18 (2002), pp. 279–284.
18. S.B. Singh and H.K.D.H. Bhadeshia, *Mater. Sci. Eng.*, 245A (1998), pp. 72–79.
19. S.S. Babu, K. Hono, and T. Sakurai, *Metall. Mater. Trans.*, 25A (1994), pp. 499–508.
20. D. Kalish and M. Cohen, *Mater. Sci. Eng.*, 6 (1970), pp. 156–166.
21. F.G. Caballero et al., *Acta Metall.*, 55 (2007), pp. 381–390.
22. K.A. Taylor et al., *Metall. Mater. Trans.*, 20A (1989), pp. 2749–2765.

F.G. Caballero, C. Garcia-Mateo, C. Capdevila, and C. Garcia de Andrés are with Centro Nacional de Investigaciones Metalúrgicas (CENIM-CSIC); Avda Gregorio del Amo, 8; Madrid, E-28040, Spain; M.K. Miller is with Oak Ridge National Laboratory, Materials Science and Technology Division, P.O. Box 2008, Oak Ridge, TN 37831-6136. Dr. Caballero can be reached at fgc@cenim.csic.es.